PCCP

Impact of Lanthanide Ion Complexation and Temperature on the Chemical Reactivity of N,N,N′,N′-tetraoctyl diglycolamide (TODGA) with the Dodecane Radical Cation

Journal:	*Physical Chemistry Chemical Physics*
Manuscript ID	CP-ART-03-2023-001119.R1
Article Type:	Paper
Date Submitted by the Author:	31-May-2023
Complete List of Authors:	Horne, Gregory; Idaho National Laboratory, Center for Radiation Chemistry Research Celis-Barros, Cristian; Colorado School of Mines, Chemistry Conrad, Jacy K; Idaho National Laboratory, Grimes, Travis; Idaho National Laboratory, Aqueous Separations and Radiochemistry Rotermund, Brian; Florida State University McLachlan, Jeffery; Lawrence Berkeley Laboratory Cook, Andrew; Brookhaven National Laboratory, Chemistry Department Mezyk, Stephen; California State University at Long Beach, Chemistry and Biochemistry

Impact of Lanthanide Ion Complexation and Temperature on the Chemical Reactivity of *N*,*N*,*N*′,*N*′-tetraoctyl diglycolamide (TODGA) with the Dodecane Radical Cation

Gregory P. Horne,[a]* Cristian Celis-Barros,[b,c] Jacy K. Conrad,[a] Travis S. Grimes,[a] Jeffery R. McLachlan,[a,e] Brian M. Rotermund,[d] Andrew R. Cook,[f] and Stephen P. Mezyk[g]*

[a] *Center for Radiation Chemistry Research, Idaho National Laboratory, Idaho Falls, ID, P.O. Box 1625, 83415, USA.*

[b] *Department of Chemistry, Colorado School of Mines, Golden, Colorado 80401, USA.*

[c] *Nuclear Science and Engineering Program, Colorado School of Mines, Golden, Colorado 80401, USA.*

[d] *Department of Chemistry and Biochemistry, Florida State University, Tallahassee, Florida 32306, USA.*

[e] *Department of Chemistry, Florida International University, Miami, Florida 33199, USA.*

[f] *Department of Chemistry, Brookhaven National Laboratory, Upton, New York, 11973, USA.*

[g] *Department of Chemistry and Biochemistry, California State University Long Beach, 1250 Bellflower Boulevard, Long Beach California, 90840-9507, USA.*

*Corresponding authors. E-mail: gregory.horne@inl.gov and stephen.mezyk@csulb.edu.

ORCID

Gregory P. Horne	0000-0003-0596-0660
Cristian Celis-Barros	0000-0002-4685-5229
Jacy K. Conrad	0000-0002-0745-588X
Travis S. Grimes	0000-0003-2751-0492
Jeffery R. McLachlan	0000-0001-6944-3377
Brian M. Rotermund	0000-0002-2379-0119
Andrew R. Cook	0000-0001-6633-3447
Stephen P. Mezyk	0000-0001-7838-1999

ABSTRACT

The impact of trivalent lanthanide ion complexation and temperature on the chemical reactivity of *N*,*N*,*N*′,*N*′-tetraoctyl diglycolamide (TODGA) with the *n*-dodecane radical cation ($RH^{\bullet+}$) has been measured by electron pulse radiolysis and evaluated by quantum mechanical calculations. Additionally, Arrhenius parameters were determined for the reaction of the non-complexed TODGA ligand with the $RH^{\bullet+}$ from 10–40 °C, giving the activation energy (E_a = 17.43 ± 1.64 kJ mol^{-1}) and pre-exponential factor (A = (2.36 ± 0.05) × 10^{13} M^{-1} s^{-1}). The complexation of Nd(III), Gd(III), and Yb(III) ions by TODGA yielded $[Ln^{III}(TODGA)_3(NO_3)_3]$ complexes that exhibited significantly increased reactivity (up to 9.3× faster) with the $RH^{\bullet+}$, relative to the non-complexed ligand: $k([Ln^{III}(TODGA)_3(NO_3)_3] + RH^{\bullet+})$ = (8.99 ± 0.93) × 10^{10}, (2.88 ± 0.40) × 10^{10},

and (1.53 ± 0.34) × 10^{10} M^{-1} s^{-1}, for Nd(III), Gd(III), and Yb(III) ions, respectively. The rate coefficient enhancement measured for these complexes exhibited a dependence on atomic number, decreasing as the lanthanide series was traversed. Preliminary reaction free energy calculations—based on a model system $[Ln^{III}(TOGDA)]^{3+}$ complex system—indicate that both electron/hole and proton transfer reactions are energetically unfavorable for complexed TODGA. Furthermore, complementary average local ionization energy calculations showed that the most reactive regions of model *N*,*N*,*N*′,*N*′-tetraethyl diglycolamide (TEDGA) complexes, $[Ln^{III}(TEGDA)_3(NO_3)_3]$, toward electrophilic attack is for the coordinated nitrate (NO_3^-) counter anions. Therefore, it is possible that radical reactions with the complexed NO_3^- counter anions dominate the differences in rates seen for the $[Ln^{III}(TODGA)_3(NO_3)_3]$ complexes, and are likely responsible for reported radioprotection in the presence of TODGA complexes.

INTRODUCTION

Understanding the impact of ionizing radiation on ligands employed for the separation, recovery, and transport of metal ions is of vital importance for the innovation of nuclear fuel cycle technologies and nuclear medicine. In both fields, novel ligands are designed to selectively form complexes with metal ions in specific oxidation states. For example, the ligand *N*,*N*,*N*′,*N*′-tetraoctyl diglycolamide (TODGA) was designed to enable the separation of the trivalent minor actinides (MA, specifically americium and curium) from the trivalent lanthanides (Ln(III)) in used nuclear fuel (UNF) reprocessing raffinates [1–15]. However, in the presence of ionizing radiation fields—for example, those arising from the radioisotopic content of UNF raffinates or from the radioactive decay of theranostic agents—these complexing ligands are subject to indirect radiolytic processes, leading to their destruction and the formation of potentially detrimental degradation products. Consequently, mastery of the radiation-induced behavior of these molecules is essential for optimizing their effectiveness and longevity, and minimizing the negative impacts of radiolysis.

The prototypical UNF reprocessing solvent, *n*-dodecane, is broken down by ionizing radiation (⇝) to form several important transient species, including the *n*-dodecane radical cation ($RH^{\bullet+}$), which reacts with ligands leading ultimately to their destruction [16–22]:

$$RH \rightsquigarrow e^-, H^\bullet, RH^{\bullet+}, R^\bullet, \quad (1)$$

$$\text{Ligand} + RH^{\bullet+} \rightarrow [\text{Ligand}]^{\bullet+}/[\text{Ligand}(+H^+)]^+ + RH/R^\bullet. \quad (2)$$

There have been extensive studies on the radiation chemistry of ligands, especially those designed for the separation and recovery of elements from UNF [23–38]. However, most contemporary investigations have focused on the radiolytic behavior of the non-complexed ligand, despite

literature precedence for their metal ion complexes exhibiting very different chemical behaviors [16,17,39–48]. For example, the complexation of trivalent iron ions (Fe(III)) by ethylenediaminetetraacetic acid (EDTA)—a typical chelation therapy ligand—was found to accelerate the rate of EDTA radiolysis, as the metal ion center provided additional inner/outer sphere reaction pathways for the products of water radiolysis [40–43]. More recently, Nd(III) and Am(III) ion complexation by TODGA in 5% 1-octanol/*n*-dodecane solvent was shown to *reduce* the extent of steady-state TODGA radiolysis and to alter the suite of degradation products, producing species that were less problematic [49]. Unfortunately, our understanding of the fundamental radiation-induced processes responsible for these divergent steady-state observations is limited, and yet it is essential for accurately predicting their behavior under real-world application conditions and to aid in the design of new radiation-resistant ligands.

Elucidation of the underpinning mechanistic changes conferred by metal ion complexation necessitates knowledge of their chemical kinetics, as recently demonstrated for the reaction of uranyl ion (UO_2^{2+}) complexes of *N*,*N*-di-(2-ethylhexyl)butyramide (DEHBA), *N*,*N*-di-2-ethylhexylisobutryamide (DEH*i*BA), and tributylphosphate (TBP) [17] with the $RH^{\bullet+}$ radical cation. In the case of DEHBA, DEH*i*BA, and TBP, the complexation of UO_2^{2+} ions by DEHBA/DEH*i*BA afforded a 2.6×/1.4× faster rate coefficient (*k*) for the reaction of the $RH^{\bullet+}$ with the corresponding complexes—$[UO_2(DEHBA)_2(NO_3)_2]$/$[UO_2(DEHiBA)_2(NO_3)_2]$—relative to the non-complexed ligands. In contrast, the complementary TBP complex—$[UO_2(TBP)_2(NO_3)_2]$—showed no change in reaction kinetics relative to non-complexed TBP [17]. These changes in the chemical reactivity of the ligand complexes were attributed to a combination of differences in reaction pathways (electron/hole transfer *vs.* proton transfer), energetics, and electron density distribution changes upon complexation [17]. Overall, these absolute kinetic measurements provided greater insight into the impact of metal ion complexation on the chemical reactivity of ligands in radiation environments.

To date, no such chemical kinetics knowledge exists for the metal ion complexes of TODGA, despite this ligand exhibiting significantly different radiolytic behavior in the presence of its MA and Ln(III) ion complexes at steady-state timescales [49]. To bridge this knowledge gap, we report here kinetic measurements demonstrating the impact of Ln(III) ion complexation on the reaction kinetics of the $RH^{\bullet+}$ with TODGA at ambient temperature (23 ± 1 °C). Further, as the real-

world application of TODGA in UNF reprocessing systems is expected to operate at temperatures above ambient (>30 ºC), Arrhenius parameters—activation energy (E_a) and pre-exponential factor (A)—were also determined for the reaction of the $RH^{\bullet+}$ with the non-complexed TODGA ligand. These kinetic data are necessary to facilitate the development of computer models to determine predicted longevity under process conditions.

METHODS

Chemicals

N,*N*,*N'*,*N'*-tetraoctyldiglycolamide (TODGA, 99%) was supplied by Technocomm Ltd (Wellbrae, Scotland, UK). Dichloromethane (DCM, ≥ 99.8%), *n*-dodecane (≥ 99% anhydrous), nitric acid (HNO_3, ≥ 99.999% trace metals basis), perchloric acid ($HClO_4$, ≥ 99.999% trace metals basis), and potassium thiocyanate (KSCN, ≥ 99.0% ACS Reagent Grade) were obtained from MilliporeSigma (Burlington, Massachusetts, USA). Nitrate salts of gadolinium (99.9%), neodymium (99.99%), and ytterbium (99.9%), were sourced from Alfa Aesar. Nitric acid (Optima Grade) was also received from Fisher Scientific. All chemicals were used without further purification. Ultra-pure water (18.2 MΩ cm) was used to prepare all aqueous solutions.

Sample Preparation

Non-complexed 100 mM TODGA ligand solutions were prepared by weighing the ligand directly into a 0.5 M DCM/*n*-dodecane stock solution. DCM was added to the *n*-dodecane solvent as a solvated electron scavenger to extend the lifetime of the $RH^{\bullet+}$ and inhibit competing reactions. A portion of this non-complexed ligand stock solution was also used for non-ambient temperature runs, following serial dilution using additional 0.5 M DCM/*n*-dodecane solution. The corresponding Ln(III) ion complex solutions were then prepared by pre-equilibrating the non-complexed TODGA ligand solution thrice with 1.0 M HNO_3 solution [50], and then contacting the acid-loaded organic phase in a 1:1 organic:aqueous ratio, with an aqueous phase comprised of ~20 mM of either Nd(III), Gd(III), or Yb(III) ions in 1.0 M HNO_3. For each contact (pre-equilibration and Ln(III) ion extraction), phases were rapidly vortex mixed for 5 minutes, and then the organic phase separated using a Thermo Scientific (Waltham, Massachusetts, USA) Sorvall Legend Centrifuge for 5 minutes at 4000 rpm. The lanthanide-loaded organic phases were then used to prepare samples for irradiation by serial dilution with additional pre-equilibrated 0.5 M

DCM/*n*-dodecane solution, maintaining a constant TODGA:Ln(III) ion ratio. The initial and post contact aqueous phases were retained for Inductively-Coupled Plasma Mass Spectrometry (ICP-MS) analyses to quantitatively determine the amount of each Ln(III) ion extracted.

Time-Resolved Electron Pulse Irradiations

Kinetics for reaction of the $RH^{\bullet+}$ with TODGA in the absence and presence of Nd(III), Gd(III), or Yb(III) ions in 0.5 M DCM/*n*-dodecane solutions at 23 ± 1 °C were measured using the Brookhaven National Laboratory (BNL) Laser Electron Accelerator Facility (LEAF) [51]. Aerated sealed samples were irradiated in static 1.00 cm Suprasil Starna Scientific Ltd. (Ilford, United Kingdom) cuvettes sealed with Teflon stoppers. Dosimetry was determined using N_2O-saturated solutions of 10 mM KSCN at $\lambda = 470$ nm ($G^*\varepsilon = 5.2 \times 10^{-4}$ m^2 J^{-1}) [52].

The time-resolved changes in the absorption decays of the $RH^{\bullet+}$ were observed near its maximum absorption at 800 nm [53] using an FND-100 silicon diode detector, and subsequently digitized using a LeCroy WaveRunner 640Zi oscilloscope (4 GHz, 8 bit). Interference filters (ca. 10 nm bandpass) were used for wavelength selection of the analyzing light. These measured $RH^{\bullet+}$ decays were fitted starting at 2 ns after the electron pulse to allow for the instrument response using a double-exponential decay function:

$$k_{obs} = \mathrm{A}_1 exp^{-k_1 t} + \mathrm{A}_2 exp^{-k_2 t} + B, \quad (3)$$

where k_{obs} was the overall rate of decay for the $RH^{\bullet+}$ signal at 800 nm, A_i are the optical density amplitudes, k_i are the pseudo-first-order rate coefficients (s^{-1}), t is time (s), and B is a baseline offset correction. The first exponential decay (A_1 and k_1 parameters) corresponds to the total reaction of the $RH^{\bullet+}$ with both the non-complexed TODGA ligand and the $[Ln^{III}(TODGA)_3(NO_3)_3]$ complex:

$$k_1 = k\mathrm{TODGA}[\mathrm{TODGA}] + k\mathrm{Complex}[\mathrm{Complex}], \quad (4)$$

while the second exponential decay (A_2 and k_2) and B variables account for the slower tailing absorption decrease seen in these systems [17].

The contribution of the non-complexed TODGA ligand (k_{TODGA}) was calculated based on its measured rate coefficient, $(9.72 \pm 6.0) \times 10^9$ M^{-1} s^{-1} [18], and its concentration, assuming a constant 3:1 TODGA:Ln(III) ion ratio complex was formed under our conditions [50,54].

Subtracting this component from the overall fitted k_1 value, and then plotting the difference as a function of solute concentration, gave the final second-order rate coefficient (k_{Complex}) values reported by this work.

Arrhenius parameters were also determined for non-complexed TODGA, wherein kinetics were measured at several temperatures (10–40 °C) in a thermostatically controlled cell holder regulated by a water bath. A thermocouple placed directly next to the cell allowed remote control of the irradiation holder temperature, stable to ± 0.1 °C. Solutions in cuvettes were cooled/pre-heated to the appropriate temperature using a bespoke sample holder supplied by the same water bath. These temperature-dependent rate coefficients allowed calculation of the activation energy (E_a, kJ mol^{-1}) and pre-exponential factor (A, M^{-1} s^{-1}) values, using the expression:

$$k = Ae^{\frac{-E^a}{RT}}, \quad (5)$$

where R is the molar gas constant (J mol^{-1} K^{-1}), and T is the absolute temperature in Kelvin (K).

The quoted rate coefficient and Arrhenius parameter errors (1σ) are a quantitative combination of measurement precision (~4%) and sample concentration (initial concentration (~8%) and dilution (<1%)) errors.

Inductively-Coupled Plasma Mass Spectrometry Metal Ion Analysis

Quantification of the amount of Ln(III) ion extracted into the organic phases was achieved by ICP-MS. Pre- and post-contact Ln(III) ion aqueous samples were digested entirely in 2% Optima grade HNO_3 and diluted, typically 100–500×. Samples were run on an Agilent (Santa Clara, CA, USA) 7500ce ICP-MS using a helium reaction cell to reduce isobaric interferences. Standard Ln(III) ion solutions were sourced from Inorganic Ventures CMS-1, instrument calibrations used SPEX CertifPrep CL-CAL-2 ICP-MS calibration standards, and the internal standard sample was 20 ppb rhodium from SPEX CertifPrep PLRH2-2Y. All standards were run at the beginning and end of each sample set measurement. Measurements were performed in triplicate and are summarized in **Table 1**.

Table 1. Results from ICP-MS analysis of the Ln(III)/1.0 M HNO_3 aqueous phases pre- and post-contact with pre-equilibrated TODGA/0.5 M DCM/*n*-dodecane organic solution. Reproducibility error in aqueous measurements was ± 5%.

Lanthanide	**[Aqueous]$_{Pre}$** (mM)	**[Aqueous]$_{Post}$** (mM)	**Δ[Aqueous] - [Organic]** (mM)
Nd(III)	19.49	7.48	12.01
Gd(III)	21.18	1.75	19.43
Yb(III)	20.00	0.38	19.62

Computations

Quantification of electronic structure computations for non-complexed TODGA and $[Ln^{III}(TODGA)]^{3+}$ in *n*-dodecane solvent used the *Gaussian16* and *Gaussview6* programs [55,56]. Geometries were determined using density functional theory (DFT) with the B3LYP functional and 6-31+g* basis set. Small corrections for dispersion effects were included using Grimme's D3 model with Becke and Johnson (BJ) damping [57]. Solvation was included in all calculations using the polarizable continuum model for *n*-dodecane, albeit solvation effects are small, as *n*-dodecane is a non-polar liquid. Computations involving a Ln(III) ion used the Stuttgart/Dresden MWB ECP/basis set with 46 core electrons. Reaction free energies for electron/hole *vs*. proton transfer from the $RH^{\bullet+}$ to TODGA, $[Ln^{III}(TODGA)]^{3+}$, HNO_3, and NO_3^- anions were determined using corrections for standard entropic states [58,59].

To further investigate the reactivity of these TODGA complexes with $RH^{\bullet+}$, we employed the Average Local Ionization Energy (ALIE) formalism [60]. The ALIE is defined as the average energy required to remove one electron from point (*r*) of a molecular space as shown by equation (6):

$$\bar{I}(r) = \frac{\sum_i \rho_i(r)|\varepsilon_i|}{\rho(r)}, \quad (6)$$

where the summation runs over all the i^{th} molecular orbital electron densities and their associated energies (ε_i), whose contribution is normalized against the total molecular electron density, $\rho(r)$. One of the advantages of analyzing ALIEs over frontier molecular orbital (FMO) methods is that they account for every possible electronic contribution to the reactivity of the molecule at a specific region in space and not solely on the highest occupied and lowest unoccupied molecular orbitals.

Another advantage of the ALIE formalism is that since $\bar{I}(r)$ is evaluated on a specific molecular contour (typically 0.0005–0.002 a.u.), it recovers chemically relevant molecular features such as atomic anisotropy, lone pairs, local polarizability, π electrons, etc., which is crucial for understanding chemical reactivity [60]. The most reactive regions on the molecule toward electrophilic reaction are those where minimum values of ALIE are found, $\bar{I}_{S,min}(r)$. Herein, we report and analyze the ALIEs projected onto the 0.0005 a.u. molecular surface of the studied TODGA complexes.

Given the size of the $[Ln^{III}(TODGA)_3(NO_3)_3]$ complexes investigated here (352 atoms), and the challenge in optimizing their geometries, we replaced the tetraoctyl chains of TODGA with tetraethyl chains, affording the *N*,*N*,*N*′,*N*′-tetraethyl diglycolamide (TEDGA) species. This simplification ensured that the calculated molecular geometries used here corresponded to a local minimum. Geometry optimizations were carried out in *ADF2019* using the *GGA* functional *PBE* along with the Slater-type orbital *TZP* basis set for all atoms [61]. Dispersion corrections were included through the Grimme's D4(EEQ) electronegativity-equilibrium method [57], while relativistic effects were included via the Zeroth-Order Relativistic Approach (ZORA) Hamiltonian [62]. The optimized molecular geometries were used to obtain the electronic structure and molecular electron densities through single point calculations using the *ORCA* software at *PBE0/DKH-def2-TZVP* level of theory for all atoms except the Ln(III) ion center, where the *SARC-DKH-TZVP* basis set was used instead [63,64]. The *MultiWFN* package was used to calculate and analyze the ALIEs [65].

RESULTS AND DISCUSSION

The temperature dependence for the reaction of $RH^{\bullet+}$ with the non-complexed TODGA ligand, along with the derived Arrhenius parameters are shown in **Figure 1**. For all investigated temperatures (10–40 °C), the rate of reaction increased with increasing temperature. The transformed Arrhenius plot gave values for the activation energy (E_a = 17.43 ± 1.64 kJ mol^{-1}) and the pre-exponential factor (A = (2.36 ± 0.05) × 10^{13} M^{-1} s^{-1}). The E_a value is consistent with previous values for biomolecular electron transfer reactions of related primary radiolysis species in water [66], but no comparative kinetic data have been reported in *n*-dodecane. Concomitant experiments for the $[Ln^{III}(TODGA)_3(NO_3)_3]$ complexes were not possible due to limitations in instrument time resolution.

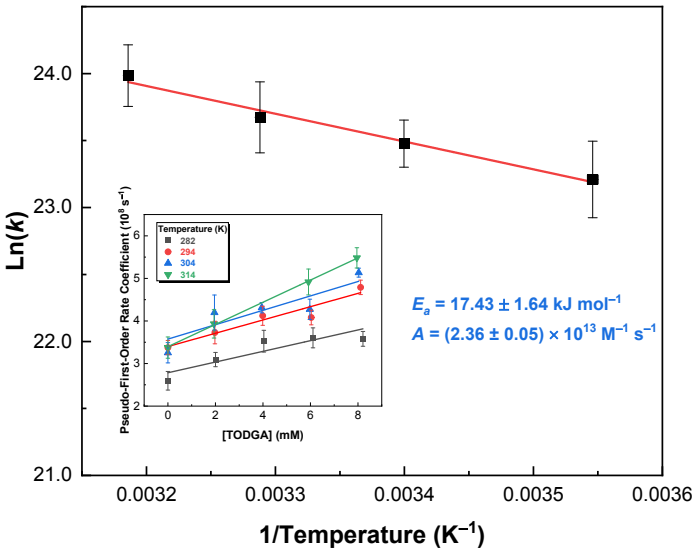

Figure 1. Arrhenius plot for the reaction of non-complexed TODGA with the $RH^{\bullet+}$ radical cation, affording an E_a = 17.43 ± 1.64 kJ mol^{-1}, and an A = (2.36 ± 0.05) × 10^{13} M^{-1} s^{-1}. Individual data points were derived from second-order rate coefficients determined at different temperatures: 10 (■), 20 (●), 30 (▲), and 40 (▼) ºC, shown in the *Inset*.

The reaction of $RH^{\bullet+}$ with the non-complexed TODGA ligand can proceed by either electron/hole or proton transfer:

$$\text{TODGA} + RH^{\bullet+} \rightarrow \text{TODGA}^{\bullet+} + RH \quad \text{(electron/hole transfer)}, \quad (7)$$

$$\rightarrow \text{TODGA}(+H^{+}) + R^{\bullet} \quad \text{(proton transfer)}, \quad (8)$$

of which the calculated reaction free energies (ΔG, eV) for these reaction pathways are -1.02 and -1.07 eV, respectively. While a full understanding of the radiation chemistry of TODGA containing solvent extraction systems requires knowledge of whether TODGA is oxidized or protonated, here we focus on the impact of metal ion complexation. Separate work seeks a fundamental understanding of the nature of the non-complexed extractant's interactions with the oxidized diluent. Both $RH^{\bullet+}$ reaction pathways are equally energetically favorable in *n*-dodecane solvent, however, we anticipate that Ln(III) ion complexation will alter the kinetic preference for these pathways, thereby influencing the rate of ligand radiolysis and the suite of associated degradation products, as demonstrated for the steady-state radiolysis of TODGA in the presence and absence of its Am(III) and Nd(III) ion complexes [49].

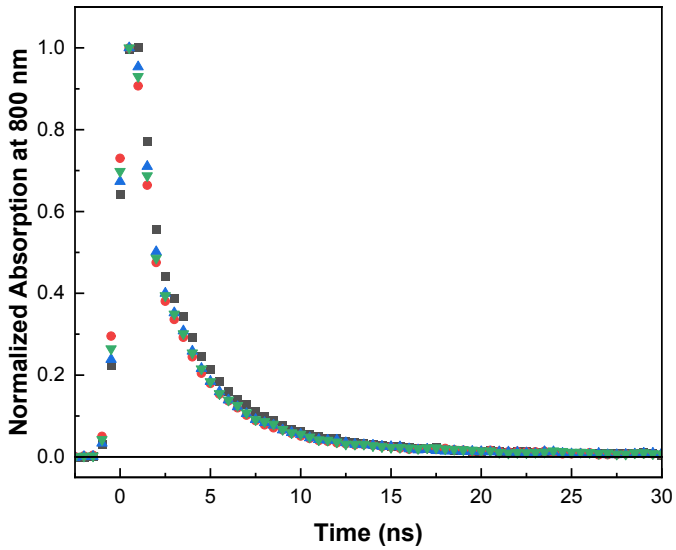

Figure 2. Normalized kinetic traces at 800 nm for electron pulse irradiated solutions of aerated 10 mM TODGA in 0.5 M DCM/*n*-dodecane without (■) and with pre-equilibration with either water (●), 1.0 M $NaNO_3$ (▲), or 1.0 M HNO_3 (▼) at 23 ± 1 °C.

Prior to performing $[Ln^{III}(TODGA)_3(NO_3)_3]$ complex reactivity measurements in *n*-dodecane, the impact of extracted water, nitrate anions (NO_3^-), and HNO_3 on the decay of the $RH^{\bullet+}$ was investigated by irradiating 10 mM TODGA in 0.5 M DCM/*n*-dodecane solutions with and without pre-equilibration with the aforementioned aqueous components. We found a negligible effect of pre-equilibration on the lifetime of the $RH^{\bullet+}$, as shown in **Figure 2**, despite complementary free energy calculations indicating that both electron/hole (-3.03 eV) and proton (-2.79 eV) transfer between $RH^{\bullet+}$ and NO_3^- anions are very favorable. These observations are consistent with the expectation that charged NO_3^- anions are negligibly extracted into the organic phase in the absence of metal ion TODGA complexes. Furthermore, our calculated reaction free energies for electron/hole (+2.26 eV) and proton (+1.59 eV) transfer between $RH^{\bullet+}$ and HNO_3 are energetically unfavorable in *n*-dodecane. However, we note that the environment around, and the form of extracted water and NO_3^-/HNO_3, is not well defined [*50*,67]. It could be more polar, thereby reducing the energy for charge/proton transfer. Nevertheless, the results in **Figure 2** suggest not enough of an effect was observed. At the low TODGA concentrations used here, micelle-like pools of extracted water [*50*,*67*] are unlikely and unsupported by our previous work that showed only 1.59 mM water uptake to the organic phase with 50 mM TODGA [68]. Therefore, the following

observed changes in kinetic behavior are attributed directly to the impact of Ln(III) ion and attendant NO_3^- anion complexation on the reactivity of the TODGA ligand with the $RH^{\bullet+}$.

Table 2. Summary of second-order rate coefficients determined for the reaction of the $RH^{\bullet+}$ radical cation with TODGA in the absence and presence of complexed lanthanides—Nd(III), Gd(III) and Yb(III) ions—in aerated 0.5 M DCM/*n*-dodecane solutions at 23 ± 1 °C.

Ligand	**Second-Order Rate Coefficient (k, × 10^{10} M^{-1} s^{-1})**			
	Non-Complexed Ligand	Nd(III) Complex	Gd(III) Complex	Yb(III) Complex
TODGA	0.97 ± 0.60 [18]	8.99 ± 0.93	2.88 ± 0.40	1.53 ± 0.34

The measured absolute second-order rate coefficients for the reaction of the $RH^{\bullet+}$ with TODGA in the absence and presence of complexed lanthanides—Nd(III), Gd(III), and Yb(III) ions—at ambient temperature are summarized in **Table 2**. For the investigated TODGA and Ln(III) ion concentration ranges, we assumed a constant TODGA:Ln(III) ion ratio of 3:1 [50], with all the $[Ln^{III}(TODGA)_3(NO_3)_3]$ complex rate coefficients given in **Table 2** calculated based on this ratio.

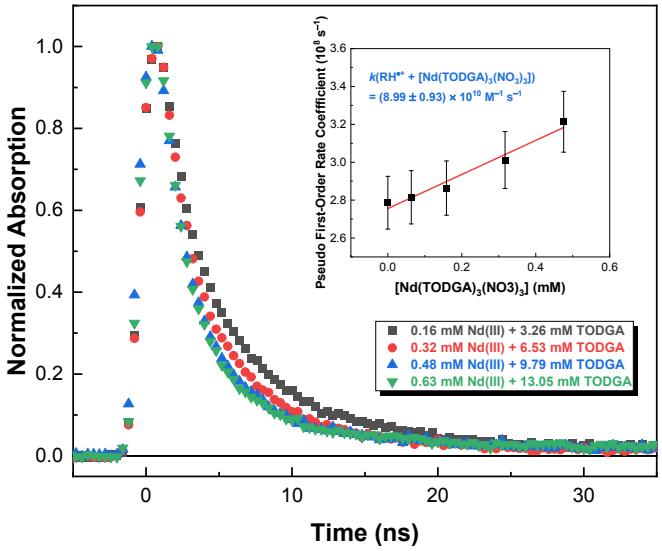

Figure 3. Normalized kinetic traces at 800 nm for electron pulse irradiated solutions of TODGA in the presence of Nd(III) ions in aerated 0.5 M DCM/*n*-dodecane at 23 ± 1 °C: 0.16 (■), 0.32 (●), 0.48 (▲), and 0.63 (▼) mM Nd(III) ions. *Inset:* Second-order determination of the rate coefficient for the reaction of $[Nd^{III}(TODGA)_3(NO_3)_3]$ with $RH^{\bullet+}$. Individual data points are the faster pseudo-first-order component of the double-exponential fit to the data shown in the main figure. The weighted linear fit corresponds to $k([Nd^{III}(TODGA)_3(NO_3)_3] + RH^{\bullet+}) = (8.99 \pm 0.93) \times 10^{10}$ M^{-1} s^{-1}.

Increasing the concentration of $[Ln^{III}(TODGA)_3(NO_3)_3]$ complexes in solution afforded a faster decay of the $RH^{\bullet+}$ absorption at 800 nm, as demonstrated by the kinetic data shown in **Figure 3** for the $[Nd^{III}(TODGA)_3(NO_3)_3]$ complex. Complementary Gd(III) and Yb(III) ion data are shown in the **Supplementary Information** (**SI**), **Figures S1** and **S2**, respectively. Fitting these decays ultimately gave the second-order rate coefficients given in **Table 2**, all of which are faster than the value for the non-complexed ligand (up to 9.3×) [18]. From a chemical kinetics perspective, the greater reactivity of the $[Ln^{III}(TODGA)_3(NO_3)_3]$ complexes, relative to the non-complexed ligand, is expected to lead to a faster rate of TODGA radiolysis. However, Kimberlin *et al.* showed that the steady-state gamma irradiation of Nd(III) and Am(III) ion complexes of TODGA decreased the rate of TODGA radiolysis and altered the suite of degradation products, relative to the non-complexed TODGA ligand [49]. These observations suggest that complexation provides an alternative reaction mechanism.

Preliminary calculations based on a model system consisting of a single TODGA molecule bound to a Ln(III) ion center with no counter NO_3^- anions ($[Ln^{III}(TOGDA)]^{3+}$, shown in **Figure S3**) indicate that both electron/hole and proton transfer reactions become unsurprisingly energetically unfavorable upon complexation. We note that the proton transfer route is especially unfavorable due to the Ln(III) ion blocking the oxygen sites which are expected to be the usual acceptors for protons in non-complexed TODGA (**Equation 8**). In the case of electron/hole transfer, the resulting $[Ln^{III}(TOGDA)]^{3+}$ complex "hole" is predicted to reside on one of the octyl chains, and not on the core of the ligand, as it does in non-complexed TODGA. The shorter octane molecule has a slightly higher ionization potential (9.80 eV [69]) than *n*-dodecane (< 9.56 eV [70,71]), which contributes to the uphill reaction energy. The values calculated for the $[Ln^{III}(TOGDA)]^{3+}$ complex suggest that an alternative pathway must be responsible for the kinetic enhancement observed here for the $[Ln^{III}(TODGA)_3(NO_3)_3]$ complexes.

To better understand the reactivity of $[Ln^{III}(TODGA)_3(NO_3)_3]$ complexes, we performed ALIE calculations for the TEDGA complex analogs, $[Ln^{III}(TEDGA)_3(NO_3)_3]$, simplifying the octyl to ethyl chains for a more reliable optimized geometry of the complexes. We evaluated the average localization energies, $\bar{I}_S(r)$, on the molecular surface to obtain a qualitative picture of the sites that are more susceptible to electrophilic reaction, whereas a quantitative analysis was performed by locating the local minima on the calculated ALIE surface, $\bar{I}_{S,min}(r)$. **Figure 4** shows

that the most reactive regions toward electrophilic attack are where the NO_3^- counter anions sit on the complex, in agreement with our previous findings for TBP [17].

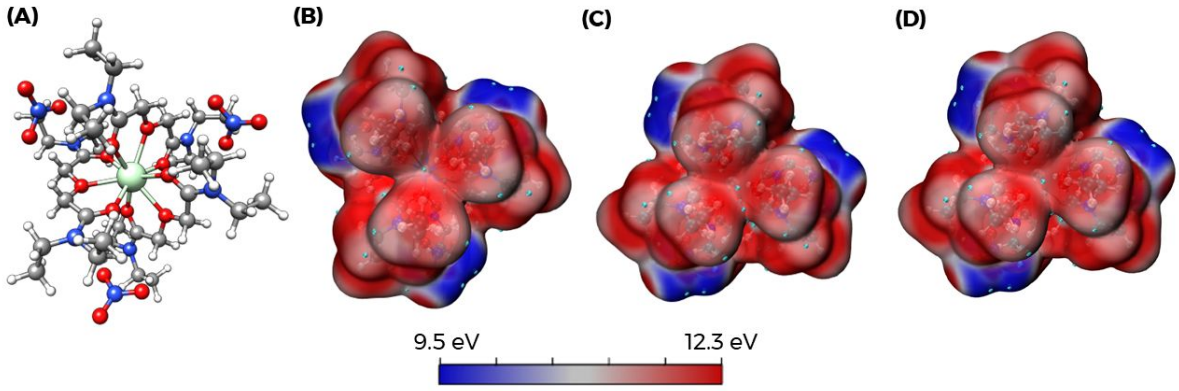

Figure 4. Molecular depiction of the studied $[Ln^{III}(TEDGA)_3(NO_3)_3]$ complex (**A**) in the same orientation as the ALIE surfaces of $[Nd^{III}(TEDGA)_3(NO_3)_3]$ (**B**), $[Gd^{III}(TEDGA)_3(NO_3)_3]$ (**C**), and $[Yb^{III}(TEDGA)_3(NO_3)_3]$ (**D**). The lowest ALIE regions are shown in blue, which indicate the least bound electron density on the molecular surface (0.0005 a.u.). Cyan dots on the surface indicate the ALIE local minima, $\bar{I}_{S,min}(r)$.

Specifically, the two O-atoms exposed to the chemical environment show two local minima with essentially equivalent average values of 8.95, 8.94, and 8.89 eV for the Nd(III), Gd(III), and Yb(III) ion TEDGA complexes, respectively, shown in **Table 3**. Interestingly, despite these being outer sphere molecules, the presence of the Ln(III) ion center causes these values to increase significantly with respect to the free NO_3^- anion in *n*-dodecane (6.48 eV, **Table 3** and **SI Figure S4**).

Table 3. ALIE minima (eV) at the 0.0005 a.u. surface of NO_3^-, TODGA, TEDGA, and the $[Ln^{III}(TEDGA)_3(NO_3)_3]$ complexes of Nd(III), Gd(III), and Yb(III) in *n*-dodecane solvent.

Moiety	**NO_3^-**	**TODGA**	**TEDGA**	**$[Ln^{III}(TEDGA)_3(NO_3)_3]$**		
				Nd(III)	Gd(III)	Yb(III)
Oxygen (NO_3^-)	6.48	-	-	8.95	8.94	8.89
Oxygen (DGA)	-	9.76	9.89	11.40	11.39	11.55
Nitrogen (DGA)	-	10.51	10.66	11.19	11.22	11.21
CH_2 (DGA)	-	10.42	10.42	11.66	11.71	11.80
CH_2 (chain)	-	10.59	11.21	11.60	11.63	11.64
CH_3	-	10.92	11.31	11.44	11.49	11.56

These ALIE findings are contrary to the Fukui function calculations reported by Kimberlin *et al.* [49]. Using *N,N,N',N'*-tetramethyl diglycolamide (TMDGA) as their computational surrogate, they found that the most likely sites for electrophilic reaction were on the methylene

CH_2-groups of the TMDGA backbone in the $[Nd^{III}(TMDGA)_3(NO_3)_3]$/$[Am^{III}(TMDGA)_3(NO_3)_3]$ complexes, and not at the coordinated NO_3^- anions. Interestingly, their corresponding calculations for coordinated chloride anions (Cl^-), $[Am^{III}(TMDGA)_3(Cl)_3]$, predicted preferential electrophilic reaction at the coordinated Cl^- anions [49]. However, given that Fukui functions are based on FMO theory, their results could be misleading in cases where molecular reactivity is not dominated by the highest-occupied (HOMO) or lowest-unoccupied (LUMO) molecular orbitals [72]. Our ALIE approach focuses on a point in space rather than a particular molecular orbital. Furthermore, assuming electron/hole transfer predominates, the direct reaction of the $RH^{\bullet+}$ with complexed NO_3^- anions generates $NO_3^\bullet$ radicals, which are likely responsible for the detection of the nitrate-containing TODGA degradation products identified by Kimberlin *et al.* These nitrate-containing degradation products were only seen for TODGA irradiated in the presence of its Nd(III) and Am(III) ion complexes [49].

In addition to the reactivity of the NO_3^- anions being altered by the presence of the Ln(III) ion center, the coordinated TEDGA ligands were found to be even more affected. **Table 3** shows the effect of complexation on the reactivity of the TEDGA ligand. The ALIE values suggest that the most reactive region toward an electrophile for non-complexed TEDGA and TODGA is around the O-atoms followed by the ethylene diglycolamide (DGA) moieties and lastly the alkyl chains. This picture is completely changed upon complexation, as the electrons around the coordinating moiety are now less susceptible to electrophilic reaction. The order of reactivity of the ligand is thus altered, with the DGA nitrogen becoming the most reactive region, though with a significantly high ALIE value of ~11.20 eV. Further changes are expected when TODGA is complexed instead of TEDGA. As observed in **Table 3**, the DGA moieties closer to the metal ion center are more notably affected upon coordination, becoming less reactive, while the increase in chain length has the opposite effect. Thus, we anticipate that in $[Ln^{III}(TODGA)_3]^{3+}$ complexes, the most reactive sites are located on the $-CH_2-$ (chain) groups and not around the DGA nitrogen atoms.

Interestingly, for all regions of the $[Ln^{III}(TEDGA)_3(NO_3)_3]$ complexes, the ALIE values increase with the atomic number of the Ln(III) ion center, which suggests that the ligand becomes less reactive as the series is traversed. This observation is consistent with the trend in rate coefficient values for the reaction of the $RH^{\bullet+}$ with the investigated $[Ln^{III}(TODGA)_3(NO_3)_3]$ complexes in **Table 2**, i.e., decreasing k with increasing lanthanide atomic number: $k([Ln^{III}(TODGA)_3(NO_3)_3] + RH^{\bullet+}) = (8.99 \pm 0.93) \times 10^{10}$, $(2.88 \pm 0.40) \times 10^{10}$, and (1.53 ± 0.34)

$\times 10^{10}$ M^{-1} s^{-1}, for Nd(III), Gd(III), and Yb(III), respectively. Our working hypothesis to explain this observation is based on the reactivity calculations performed and the fact that the effective nuclear charge increases as the lanthanide series is traversed [73], thereby affecting more significantly the electronic structure and reactivity of the coordinated ligands of the heavier Ln(III) ion complexes over the outer sphere NO_3^- anions (**Table 3**). Thus, the trend in kinetics would be observed not due to the reaction between the $RH^{\bullet+}$ with NO_3^- anions, but rather due to secondary reactions between the resulting $NO_3^\bullet$ radicals and coordinated TODGA molecules, which is where the decreased reactivity is observed. Follow up calculations are underway to explore this hypothesis.

CONCLUSIONS

Complexation of Ln(III) ions by TODGA afforded complexes with increased chemical reactivity (up to 9.3×) towards the $RH^{\bullet+}$ formed in *n*-dodecane radiolysis. Further, the $[Ln^{III}(TODGA)_3(NO_3)_3]$ complexes exhibited reaction rates that decreased as the lanthanide series was traversed—Nd(III) to Gd(III) to Yb(III)—indicating a change in reaction mechanism upon metal ion complexation. However, these enhanced reaction rates with the $RH^{\bullet+}$ do not necessarily translate to more extensive TODGA radiolysis, as evident from previous work by Kimberlin *et al.* [49].

Our reaction free energy calculations showed that electron/hole and proton transfer were both energetically favorable for the reaction of $RH^{\bullet+}$ with non-complexed TODGA, but become highly uphill for a model $[Ln^{III}(TOGDA)]^{3+}$ complex in *n*-dodecane solvent, suggesting another reason for the enhanced rates with the complexes. Complementary ALIE calculations demonstrated that the most susceptible sites to electrophilic reaction are on the O-atoms of the coordinated NO_3^- anions in all three $[Ln^{III}(TODGA)_3(NO_3)_3]$ complexes. Consequently, while enhanced reaction rates appeared to implicate differences in the chemical reactivity of the TODGA ligand, one must also consider the impact of the attendant NO_3^- counter anions. The reaction of non-complexed NO_3^- anions with the $RH^{\bullet+}$ were predicted to be energetically favorable (< -2.79 eV), and likely also influenced by the charge density of the bound Ln(III) ion, thereby also providing a plausible explanation for the change in $[Ln^{III}(TODGA)_3(NO_3)_3]$ complex reactivity as the lanthanide series is traversed. Overall, it is possible that radical reactions with the NO_3^- counter

anions dominate the differences in rates we see with the $[Ln^{III}(TODGA)_3(NO_3)_3]$ complexes, as found for UO_2^{2+} complexes of TBP [17].

Although the presented computational models suggest that the reaction between the $RH^{\bullet+}$ and the $[Ln^{III}(TODGA)_3(NO_3)_3]$ complexes takes place where the NO_3^- counter anions are located, the coordinated ligands may still be subject to subsequent radiation-induced reactions with the initial $NO_3^\bullet$ radical product, assuming electron/hole transfer predominates. The fact that the alkyl chain is subject to less electronic reorganization upon coordination, it provides a possible candidate for reactive sites in addition to the NO_3^- counter anions. Conversely, the $NO_3^\bullet$ radical (electron/hole transfer) is neutral and on the relative outskirts of the complex. Thus, the $NO_3^\bullet$ radical may be liable to diffuse away from the complex and react with the more abundant molecules of the solvent, i.e., *n*-dodecane, thereby shifting any potential sequential damage away from TODGA. Follow up quantum mechanical calculations are underway to evaluate the chemical behavior and fate of complexed $NO_3^\bullet$ radicals as well as the reactivity of the actual lanthanide complexed with TODGA.

CONFLICTS OF INTEREST

There are no conflicts to declare.

ASSOCIATED CONTENT

Supplementary Information for *Gd(III) and Yb(III) TODGA Complex Reaction Kinetic Data, Geometry Optimized Molecular Structure for* $[Ln^{III}(TODGA)]^{3+}$ *Complex*, *Geometry Optimized Bond Lengths for* $[Ln^{III}(TEDGA)_3(NO_3)_3]$ *Complexes,* and additional *ALIE Calculations for Non-Complexed Diglycolamide Molecules and* NO_3^- *Anions*.

AUTHOR INFORMATION

Corresponding Authors

Gregory P. Horne – Center for Radiation Chemistry Research, Idaho National Laboratory, 1955 N. Freemont Ave., Idaho Falls, 83415, USA; orcid.org/0000-0003-0596-0660; E-mail: gregory.horne@inl.gov.

Stephen P. Mezyk – Department of Chemistry and Biochemistry, California State University Long Beach, 1250 Bellflower Boulevard, Long Beach California, 90840-9507, USA.; orcid.org/0000-0001-7838-1999; E-mail: stephen.mezyk@csulb.edu.

ACKNOWLEDGEMENTS

This research has been funded by the U.S. Department of Energy Assistant Secretary for Nuclear Energy, under the Material Recovery and Waste Form Development Campaign, DOE-Idaho Operations Office Contract DE-AC07-05ID14517. Cook and electron pulse irradiation experiments at the LEAF of the BNL Accelerator Center for Energy Research were supported by the U.S. Department of Energy, Office of Basic Energy Sciences, Division of Chemical Sciences, Geosciences, and Biosciences under contract DE-SC0012704. McLachlan thanks the U.S. DOE Office of Science, Office of Workforce Development for Teachers and Scientists, Office of Science Graduate Student Research (SCGSR) program for supporting his contributions to this work.

REFERENCE

(1) Y. I. Sasaki and G.R. Choppin, Solvent extraction of Eu, Th, U, Np and Am with N,N'-dimethyl-N,N'-dihexyl-3-oxapentanediamide and its analogous compounds. *Anal. Sci.*, **1996**, *12*, 225–230.

(2) Y. Sasaki and G.R. Choppin, Extraction of Np(V) by N,N'-dimethyl-N,N'-dihexyl-3-oxapentanediamide. *Radiochim. Acta*, **1998**, *80*, 85–88.

(3) Y. Sasaki, Y. Sugo, S. Suzuki, and S. Tachimori, The novel extractants, diglycolamides, for the extraction of lanthanides and actinides in HNO_3-*n*-dodecane system. *Solvent Extr. Ion Exch.*, **2001**, *19* , 91–103.

(4) S. Tachimori, Y. Sasaki, and S. Suzuki, Modification of TODGA-n-dodecane solvent with a monoamide for high loading of lanthanides(III) and actinides(III). *Solvent Extr. Ion Exch.*, **2002**, *20*, 687–699.

(5) A. Geist, U. Mullich, D. Magnusson, P. Kaden, G. Modolo, A. Wilden, and T. Zevaco, Actinide(III)/Lanthanide(III) Separation Via Selective Aqueous Complexation of Actinides(III) using a Hydrophilic 2,6-Bis(1,2,4-Triazin-3-Yl)-Pyridine in Nitric Acid. *Solvent Extr. Ion Exch.*, **2012**, *30*, 433–444.

(6) K. Bell, C. Carpentier, M. Carrott, A. Geist, C. Gregson, X. Heres, D. Magnusson, R. Malmbeck, F. McLachlan, G. Modolo, U. Mullich, M. Sypula, R. Taylor, and A. Wilden, Progress towards the development of a new GANEX process. *Procedia Chem.*, **2012**, *7*, 392–397.

(7) J. Brown, F. McLachlan, M. Sarsfield, R. Taylor, G. Modolo, and A. Wilden, Plutonium Loading of Prospective Grouped Actinide Extraction (GANEX) Solvent Systems based on Diglycolamide Extractants. *Solvent Extr. Ion Exch.*, **2012**, 30, 127–141.

(8) S.A. Ansari, P. Pathak, P.K. Mohapatra, and V.K. Manchanda, Chemistry of Diglycolamides: Promising Extractants for Actinide Partitioning. *Chem. Rev.*, **2012**, *112*, 1751–1772.

(9) M.J. Carrot, C.R. Gregson, and R.J. Taylor, Neptunium Extraction and Stability in the GANEX Solvent: 0.2 M TODGA/0.5 M DMDOHEMA/Kerosene. *Solvent Extr. Ion Exch.*, **2013**, 31, 463–482.

(10) G. Modolo, A. Wilden, P. Kaufholz, D. Bosbach, and A. Geist, Development and demonstration of innovative partitioning processes (i-SANEX and 1-cycle SANEX) for actinide partitioning. *Prog. Nucl. Energy*, **2014**, *72*, 107–114.

(11) A. Wilden, G. Modolo, P. Kaufholz, F. Sadowski, S. Lange, M. Sypula, D. Magnusson, U. Mullich, A. Geist, and D. Bosbach, Laboratory-Scale Counter-Current Centrifugal Contactor Demonstration of an Innovative-SANEX Process Using a Water Soluble BTP. *Solvent Extr. Ion Exch.*, **2015**, *33*, 91–108.

(12) M. Carrott, A. Geist, X. Hères, S. Lange, R. Malmbeck, M. Miguirditchian, G. Modolo, A. Wilden, and R. Taylor, Distribution of plutonium, americium and interfering fission products between nitric acid and a mixed organic phase of TODGA and DMDOHEMA in kerosene, and implications for the design of the "EURO-GANEX" process. *Hydrometallurgy*, **2015**, *152*, 139–148.

(13) D. Whittaker, A. Geist, G. Modolo, R. Taylor, M. Sarsfield, and A. Wilden, Applications of Diglycolamide Based Solvent Extraction Processes in Spent Nuclear Fuel Reprocessing, Part 1: TODGA. *Solvent Extr. Ion Exch.*, **2018**, *36*, 223–256.

(14) R. Malmbeck, D. Magnusson, S. Bourg, M. Carrott, A. Geist, X. Heres, M. Miguirditchian, G. Modolo, U. Mullich, C. Sorel, R. Taylor, and A. Wilden, Homogenous recycling of transuranium elements from irradiated fast reactor fuel by the EURO-GANEX solvent extraction process. *Radiochim. Acta*, **2019**, *107*, 917–929.

(15) C. Marie, P. Kaufholz, V. Vanel, M.-T. Duchesne, E. Russello, F. Faroldi, L. Baldini, A. Casnati, A. Wilden, G. Modolo, and M. Miguirditchian, Development of a Selective Americium Separation Process Using H4TPAEN as Water-Soluble Stripping Agent*Solvent Extr. Ion Exch.*, **2019**, *37*, 313–327.

(16) T. Toigawa, D.R. Peterman, D.S. Meeker, T.S. Grimes, P.R. Zalupski, S.P. Mezyk, A.R. Cook, S. Yamashita, Y. Kumagai, T. Matsumura, and G.P. Horne, Radiation-Induced Effects on the Extraction Properties of Hexa-n-octylnitrilo-triacetamide (HONTA) Complexes of Americium and Europium. *Phys. Chem. Chem. Phys.*, **2021**, *23*, 1343–1351.

(17) C. Celis-Barros, C.D. Pilgrim, A.R. Cook, T.S. Grimes, S.P. Mezyk, and G.P. Horne, Influence of Uranyl Complexation on the Reaction Kinetics of the Dodecane Radical Cation with Used Nuclear Fuel Extraction Ligands (TBP, DEHBA, and DEHiBA). *Physical Chemistry and Chemical Physics*, **2021**, *23*, 24589–24597.

(18) C.A. Zarzana, G.S. Groenewold, B.J. Mincher, S.P. Mezyk, A. Wilden, H. Schmidt, G. Modolo, J.F. Wishart, and A.R. Cook, A Comparison of the γ-Radiolysis of TODGA and T(EH)DGA Using UHPLC-ESI-MS Analysis. *Solv. Extr. Ion Exch.*, **2015**, *33 (5)*, 431–447.

(19) S.P. Mezyk, B.J. Mincher, S.B. Dhiman, B. Layne and J.F. Wishart, The role of organic solvent radical cations in separations ligand degradation. *J. Radioanal. Nucl. Chem.*, **2016**, *307 (3)*, 2445–2449.

(20) S.P. Mezyk, G.P. Horne, B.J. Mincher, P.R. Zalupski, A.R. Cook, and J.F. Wishart, The Chemistry of Separations Ligand Degradation by Organic Radical Cations. *Proc. Chem.*, **2016**, *21*, 61–65.

(21) J. Drader, G. Saint-Louis, J.M. Muller, M.-C. Charbonnel, P. Guilbaud, L. Berthon, K.M. Roscioli-Johnson, C.A. Zarzana, C. Rae, G.S. Groenewold, B.J. Mincher, S.P. Mezyk, K. McCann, S.G. Boyes, and J. Braley, Radiation chemistry of the branched-chain monoamide di-2-ethylhexyl-isobutyramide. *Solv. Extr. Ion Exch.*, **2017**, *35 (7)*, 480–495.

(22) G.P. Horne, C.A. Zarzana, T.S. Grimes, C. Rae, J. Ceder, S.P. Mezyk, B.J. Mincher, M.-C. Charbonnel, P. Guilbaud, G. Saint-Louis, and L. Berthon, Effect of chemical environment on the radiation chemistry of N,N-di-(2-ethylhexyl)butyramide (DEHBA) and plutonium retention. *Dalton Trans.*, **2019**, *48*, 14450–14460.

(23) B.J. Mincher and S.P. Mezyk, Radiation Chemical Effects on Radiochemistry: A Review of Examples Important to Nuclear Power. *Radiochim. Acta*, **2009**, *97*, 519–534.

(24) B.J. Mincher, G. Modolo, and S.P. Mezyk, Review Article: The Effects of Radiation Chemistry on Solvent Extraction: 1. Conditions in Acidic Solution and a Review of TBP Radiolysis. *Solv. Extr. Ion Exch.*, **2009a**, *27 (1)*, 1–25.

(25) B.J. Mincher, G. Modolo, and S.P. Mezyk, Review Article: The Effects of Radiation Chemistry on Solvent Extraction: 2. A Review of Fission-Product Extraction. *Solv. Extr. Ion Exch.*, **2009b**, *27 (3)*, 331–353.

(26) B.J. Mincher, G. Modolo, and S.P. Mezyk, Review Article: The Effects of Radiation Chemistry on Solvent Extraction 3: A Review of Actinide and Lanthanide Extraction. *Solv. Extr. Ion Exch.* **2009c**, *27 (5–6)*, 579–606.

(27) L. Berthon and M.-C. Charbonnel, Chapter 8 Radiolysis of Solvents Used in Nuclear Fuel Reprocessing, Ion Exchange and Solvent Extraction: A Series of Advances, Volume 19, B.A. Moyer (Editor), 429–514.

(28) R. Malmbeck and N. L. Banik, Radiolytic behavior of a TODGA based solvent under alpha irradiation. *J. Radioanal. Nucl. Chem.*, **2020**, *326*, 1609–1615.

(29) H. Galan, C.A. Zarzana, A. Wilden, A. Nunez, H. Schmidt, R.J.M. Egberink, A. Leoncini , J. Cobos , W. Verboom , G. Modolo , G. S. Groenewold and B. J. Mincher , Gamma-radiolytic stability of new methylated TODGA derivatives for minor actinide recycling. *Dalton Trans.*, **2015**, *44*, 18049–18056.

(30) V. Hubscher-Bruder, V. Mogilireddy, S. Michel, A. Leoncini, J. Huskens, W. Verboom, H. Galan, A. Nunez, J. Cobos, G. Modolo, A. Wilden, H. Schmidt, M.C.

Charbonnel, P. Guilbaud, and N. Boubals, Behaviour of the extractant Me-TODGA upon gamma irradiation: quantification of degradation compounds and individual influences on complexation and extraction. *New J. Chem.*, **2017**, *41*, 13700–13711.

(31) H. Galan, A. Nunez, A.G. Espartero, R. Sedano, A. Durana, and J. de Mendoza, Radiolytic stability of TODGA: Characterization of degraded samples under different experimental conditions. *Proc. Chem.*, **2012**, *7*, 195–201.

(32) C.A. Zarzana, G.S. Groenewold, B.J. Mincher, S.P. Mezyk, A. Wilden, H. Schmidt, G. Modolo, J.F. Wishart, and A.R. Cook, A Comparison of the γ-Radiolysis of TODGA and T(EH)DGA Using UHPLC-ESI-MS Analysis. *Solvent Extr. Ion Exch.*, **2015**, *33* , 431–447.

(33) K.M. Roscioli-Johnson, C.A. Zarzana, G.S. Groenewold, B.J. Mincher, A. Wilden, H. Schmidt, G. Modolo, and B. Santiago-Schübel, A Study of the Radiolysis of N,N-Didodecyl-N',N'-Dioctyldiglycolamide Using UHPLC-ESI-MS Analysis. *Solvent Extr. Ion Exch.*, **2016**, *34*, 439–453.

(34) I. Sánchez-García, H. Galán, J.M. Perlado, and J. Cobos, Stability studies of GANEX system under different irradiation conditions. *EPJ Nuclear Sci. Technol.*, **2019**, *5*, 19–26.

(35) I. Sanchez-Garcia, H. Galan, J.M. Perlado, and J. Cobos, Development of experimental irradiation strategies to evaluate the robustness of TODGA and water-soluble BTP extraction systems for advanced nuclear fuel recycling. *Radiat. Phys. Chem.*, **2020**, *177* , 109094.

(36) Y. Wang, Y. Wan, Y. Cai, L. Yuan, W. Feng, and N. Liu, A review of the alpha radiolysis of extractants for actinide lanthanide separation in spent nuclear fuel reprocessing. *Radiochim. Acta*, **2021**, *109*, 603–623.

(37) Y. Sugo , M. Taguchi , Y. Sasaki , K. Hirota and T. Kimura , Radiolysis study of actinide complexing agent by irradiation with helium ion beam. *Radiat. Phys. Chem.*, **2009**, *78*, 1140–1144.

(38) Y. Sugo, Y. Sasaki, M. Taguchi, and N.S. Ishioka, α-Radiation effect on solvent extraction of minor actinide. *J. Radioanal. Nucl. Chem.*, **2015**, *303*, 1381–1384.

(39) G.V. Buxton and R.M. Sellers, The radiation chemistry of metal ions in aqueous solution. *Coord. Chem. Rev.*, **1977**, *22 (3)*, 195–274.

(40) S.N. Bhattacharyya and K.P. Kundu, The radiation chemistry of aqueous solutions of ferric ethylenediamine tetraacetate. *Int. J. Radiat. Phys. Chem.*, **1971**, *3*, 1–10.

(41) K.P. Kundu and N. Matuura, Gamma-radiolysis of ferric ethylene diamine tetra-acetate in neutral aqueous solution. *Int. J. Radiat. Phys. Chem.*, **1975**, *7*, 565–571.

(42) G.R. Buettner, T.P. Doherty, and L.K. Patterson, The kinetics of the reaction of superoxide radical with iron(III) complexes of EDTA, DETAPAC and HEDTA. *FEBS Lett.*, **1983**, *158*, 143–146.

(43) Y.A. Ilan and G. Czapski, The reaction of superoxide radical with iron complexes of EDTA studied by pulse radiolysis. *Biochimica et Biophysica Acta*, **1977**, *498*, 386–394.

(44) B.K. Sharma and R. Gupta, γ-Radiolysis of aqueous solutions of cerium(III)-ethylenediamine tetraacetate. *Radiat. Eff. Lett.*, **1980**, *57*, 149–154.

(45) B.K. Sharma and R. Gupta, On the γ-radiolysis of aqueous solution of cerium(III) nitriloltriacetate *Radiat. Phys. Chem.*, **1984**, *24*, 233–237.

(46) M.M. Khater, I.M. Kenawi, A.M. Atwa, and M. B. Hafez, Radiolysis of NTA complexes with uranium(VI), iron(III) and nickel(II). *J. Radioanal. Nucl. Chem.*, **1987**, *111*, 17–26.

(47) N.E. Bibler, Gamma and alpha radiolysis of aqueous solutions of diethylenetriaminepentaacetic acid. *J. Inorg. Nucl. Chem.*, **1972**, *34*, 1417–1425.

(48) M.B. Hafez, H. Roushdy, and N. Hafez, Radiolysis of aqueous solutions of ethylenediaminetetraacetatocerium(III). *J. Radioanal. Chem.*, 1978, **43** , 121–129.

(49) A. Kimberlin, G. Saint-Louis, D. Guillaumont, B. Camès, P. Guilbaud, and L. Berthon, Effect of metal complexation on diglycolamide radiolysis: a comparison between ex situ gamma and in situ alpha irradiation. *Phys. Chem. Chem. Phys.*, **2022**, *24*, 9213–9228.

(50) M.P. Jensen, T. Yaita, and R. Chiarizia, Reverse-Micelle Formation in the Partitioning of Trivalent f-Element Cations by Biphasic Systems Containing a Tetraalkyldiglycolamide. *Langmuir*, **2007**, *23 (9)*, 4765–4774.

(51) J.F. Wishart, A.R. Cook, and J.R. Miller, The LEAF picosecond pulse radiolysis facility at Brookhaven National Laboratory. *Rev. Sci. Instr.*, **2004**, *75 (11)*, 4359–4366.

(52) G.V. Buxton and C.R. Stuart, Re-evaluation of the thiocyanate dosimeter for pulse radiolysis. *J. Chem. Soc. Faraday Trans.*, **1995**, *92*, 279–281.

(53) R. Mehnert, O. Brede, and W. Naumann, *Ber. Bunsenges. Phys. Chem.* **1984**, *88*, 71–80.

(54) T. Fujii, K. Aoki, and H. Yamana, Effect of Nitric Acid Distribution on Extraction Behavior of Trivalent F-Elements in a TRUEX System. *Solv. Extr. Ion Exch.* **2006**, *24 (3)*, 347–357.

(55) M.J. Frisch, G.W. Trucks, H.B. Schlegel, G.E. Scuseria, M.A. Robb, J.R. Cheeseman, G. Scalmani, V. Barone, G.A. Petersson, H. Nakatsuji, X. Li, M. Caricato, A.V. Marenich, J. Bloino, B.G. Janesko, R. Gomperts, B. Mennucci, H.P. Hratchian, J.V. Ortiz, A.F. Izmaylov, J.L. Sonnenberg, D. Williams-Young, F. Ding, F. Lipparini, F. Egidi, J. Goings, B. Peng, A. Petrone, T. Henderson, D. Ranasinghe, V.G. Zakrzewski, J. Gao, N. Rega, G. Zheng, W. Liang, M. Hada, M. Ehara, K. Toyota, R. Fukuda, J. Hasegawa, M. Ishida, T. Nakajima, Y. Honda, O. Kitao, H. Nakai, T. Vreven, K. Throssell, J.A. Montgomery, J.E. Peralta, F. Ogliaro, M.J. Bearpark, J.J. Heyd, E.N. Brothers, K.N. Kudin, V.N. Staroverov, T.A. Keith, R. Kobayashi, J. Normand, K. Raghavachari, A.P. Rendell, J.C. Burant, S.S. Iyengar, J. Tomasi, M. Cossi, J.M. Millam, M. Klene, C. Adamo, R. Cammi, J.W. Ochterski, R.L. Martin, K. Morokuma, O. Farkas, J.B. Foresman, and D.J. Fox, Gaussian 16, Revision A.03, Gaussian, Inc., Wallingford CT, **2016**.

(56) R. Dennington, T. Keith, and J. Millam, GaussView, Version 6.1.1, Release notes. Semichem Inc., Shawnee Mission, KS, **2019**.

(57) S. Grimme, S. Ehrlich, and L. Goerigk, Effect of the damping function in dispersion corrected density functional theory. *Comp. Chem.* **2011**, *32* (7), 1456–1465.

(58) C.P. Kelly, C.J. Cramer, and D.G. Truhlar, Aqueous Solvation Free Energies of Ions and Ion-Water Clusters Based on an Accurate Value for the Absolute Aqueous Solvation Free Energy of the Proton. *J. Phys. Chem. B*, **2006**, *110 (32)*, 16066–16081.

(59) C.P. Kelly, C.J. Cramer, and D. G. Truhlar, Single-Ion Solvation Free Energies and the Normal Hydrogen Electrode Potential in Methanol, Acetonitrile, and Dimethyl Sulfoxide. *J. Phys. Chem. B*, **2007**, *111 (2)*, 408–422.

(60) P. Politzer, J.S. Murray, and F.A. Bulat. Average local ionization energy: a review. *J. Mol. Mod.* **2010**, *16 (11)*, 1731–1742.

(61) G. te Velde, F.M. Bickelhaupt, E.J. Baerends, C. Fonseca Guerra, S.J.A. van Gisbergen, J.G. Snijders, and T. Ziegler, Chemistry with ADF. *J. Comp. Chem.* **2001**, *22 (9)*, 931–967.

(62) E. van Lenthe, E.-J. Baerends, and J.G. Snijders. Relativistic regular two-component Hamiltonians. *J. Chem. Phys.* **1993**, *99.6*, 4597–4610.

(63) F. Neese, The ORCA program system. *Wiley Interdisciplinary Reviews: Comp. Mol. Sci.* **2012**, *2 (1)*, 73–78.

(64) F. Neese, Software update: the ORCA program system, version 4.0. *Wiley Interdisciplinary Reviews: Comp. Mol. Sci.* **2018**, 8 (1), e1327.

(65) T. Lu and F. Chen., Multiwfn: A multifunctional wavefunction analyzer. *J. Comp. Chem.* **2012**, *33 (5)*, 580–592.

(66) G.V. Buxton, C.L. Greenstock, W.P. Helman, and A.B. Ross, Critical review of rate constants for reactions of hydrated electrons, hydrogen atoms and hydroxyl radicals (•OH/•O$^-$) in aqueous solution. *J. Phys. Chem. Ref. Data*, **1988**, *17*, 513–886.

(67) S. Nave, G. Modolo, and C. Madic, Aggregation Properties of N,N,N′,N′-Tetraoctyl-3-oxapentanediamide (TODGA) in *n*-Dodecane. *Solv. Extr. Ion Exch.* **2004**, *22 (4)*, 527–551.

(68) G.P. Horne, C.A. Zarzana, C. Rae, A.R. Cook, S.P. Mezyk, P.R. Zalupski, A. Wilden, and B.J. Mincher, Does addition of 1-octanol as a phase modifier provide radical scavenging radioprotection for N,N,N′,N′-tetraoctyldiglycolamide (TODGA)? *Phys. Chem. Chem. Phys.* **2020**, *22*, 24978–24985.

(69) https://webbook.nist.gov/cgi/cbook.cgi?Name=octane&Units=SI&cIE=on, last accessed 09/20/2022.

(70) https://webbook.nist.gov/cgi/cbook.cgi?Name=undecane&Units=SI&cIE=on, last accessed 09/20/2022.

(71) S.G. Lias, "Ionization Energy Evaluation" in NIST Chemistry WebBook, NIST Standard Reference Database Number 69, Eds. P.J. Linstrom and W.G. Mallard, National Institute of Standards and Technology, Gaithersburg MD, 20899.

(72) F.A. Bulat, J.S. Murray, and P. Politzer, Identifying the most energetic electrons in a molecule: The highest occupied molecular orbital and the average local ionization energy. *Comp. Theor. Chem.* **2021**, *1199*, 113192.

(73) K.N. Raymond, D.L. Wellman, C. Sgarlata, and A.P. Hill, Curvature of the lanthanide contraction: An explanation. *Comptes Rendus Chimie* **2010**, *13 (6–7)*, 849–852.